The Isthmic Nuclei Providing Parallel Feedback Connections to the Avian Tectum Have Different Neurochemical Identities: Expression of Glutamatergic and Cholinergic Markers in the Chick (*Gallus gallus*)

Cristian González-Cabrera,[1]* Florencia Garrido-Charad,[1] Alejandro Roth,[1] and Gonzalo J. Marín[1,2]*

[1]Department of Biology, Faculty of Sciences, University of Chile, Santiago, Chile
[2]Faculty of Medicine, University Finis Terrae, Santiago, Chile

ABSTRACT

Retinal inputs to the optic tectum (TeO) triggered by moving stimuli elicit synchronized feedback signals from two isthmic nuclei: the isthmi parvocelullaris (Ipc) and isthmi semilunaris (SLu). Both of these nuclei send columnar axon terminals back to the same tectal position receiving the retinal input. The feedback signals from the Ipc seem to act as an attentional spotlight by selectively boosting the propagation of retinal inputs from the tectum to higher visual areas. Although Ipc and SLu nuclei are widely considered cholinergic because of their immunoreactivity for choline acetyltransferase (ChAT), contradictory findings, including the expression of the vesicular glutamate transporter 2 (VGluT2) mRNA in Ipc neurons, have raised doubts about the purely cholinergic nature of this nucleus. In this study, in chicks, we revise the neurochemical identity of the isthmic nuclei by using in situ hybridization assays for VGluT2 along with three cholinergic markers: the vesicular acetylcholine transporter (VAChT), the high-affinity choline transporter (CHT1) and ChAT. We found that neurons in the SLu showed strong mRNA expression of all three cholinergic markers, whereas the expression of VAChT mRNA in the Ipc was undetectable in our essays. Instead, Ipc neurons exhibited a strong expression of VGluT2 mRNA. Immunohistochemistry assays showed VGluT2 immunoreactivity in the TeO codistributing with anterogradely labeled Ipc axon-terminal boutons, further supporting a glutamatergic function for the Ipc nucleus. Therefore, our results strongly suggest that, in the chick, whereas the feedback from the SLu to the TeO is indeed cholinergic, the feedback from the Ipc has a marked glutamatergic component. J. Comp. Neurol. 523:1341–1358, 2015.

INDEXING TERMS: nucleus isthmi; tectofugal pathway; spatial attention; neurochemical identity; RRID:nlx_84100; RRID:nlx_84530; RRID:OMICS_02343; RRID:AB_514497; RRID:AB_2315140; RRID:AB_2239153; RRID:AB_90661; RRID:AB_2313581; RRID:AB_2336126; RRID:AB_10562420; RRID:AB_10562715; RRID: nif-0000–24345

The tectofugal pathway has been long recognized as a principal visual pathway in birds, as it routes the majority of retinal input to higher visual areas (Karten and Revzin, 1966; Hunt and Webster, 1975; Benowitz and Karten, 1976; Mpodozis et al., 1995). Its main visual center, the optic tectum (TeO; superior colliculus in mammals), is highly differentiated, encompassing intricate neural circuits that mediate eye/head orientation, avoidance reactions, visual discriminative behaviors, and spatial attention (Bischof and Watanabe, 1997; Nguyen et al., 2004; Knudsen, 2007; Wylie et al., 2009;

Additional Supporting Information may be found in the online version of this article.

Grant sponsor: Chilean National Fund for Scientific and Technological Research (FONDECYT); Grant number: 1110281 (to G.M.) 1080252 (to A.R.).

*CORRESPONDENCE TO: Cristian González-Cabrera and Gonzalo J. Marín, Departamento de Biología, Facultad de Ciencias, Universidad de Chile, Las Palmeras 3425, Ñuñoa, Santiago, Chile.
E-mail: cristian.gonzalez.ca@gmail.com and gmarin@uchile.cl.

Received September 15, 2014; Revised December 24, 2014;
Accepted December 25, 2014.
DOI 10.1002/cne.23739
Published online March 12, 2015 in Wiley Online Library (wileyonlinelibrary.com)

Marín et al., 2012). Retinal fibers terminate in the superficial tectal layers forming a topographic map of the contralateral visual field (Ramón y Cajal, 1911; Hunt and Webster, 1975; Angaut and Repérant, 1976), whereas the ascending tectofugal output stems from tectal ganglion cells (TGCs) located in layer 13 (Benowitz and Karten, 1976; Karten et al., 1997). The TGCs have wide dendritic fields with characteristic terminal specializations distributed within a single tectal layer, which is specific for different TGC types (Luksch et al., 1998, 2001). The different TGCs form parallel channels that terminate in specific subdivisions in the nucleus rotundus (Rt; caudal pulvinar in mammals) of the thalamus (Benowitz and Karten, 1976; Mpodozis et al., 1996; Karten et al., 1997; Hellmann and Güntürkün, 2001; Marín et al., 2003).

The ascending tectofugal output is controlled by the nuclei of the isthmic complex, the isthmi pars parvocellularis (Ipc), the isthmi pars Semilunaris (SLu), and the isthmi pars magnocellularis (Imc) (Wang et al., 2006; Marín et al., 2007, 2012). "Shepherd-crook" neurons from tectal layer 10 carry retinal inputs to these nuclei via topographically organized axons. Neurons from the Ipc and the SLu feedback to the TeO via columnar axons arranged in a "homotopic" fashion, such that the signals from both nuclei reach the same tectal position from which the retinal input originates (Hunt et al., 1977; Güntürkün and Remy, 1990; Wang et al., 2006). Imc neurons provide widespread "heterotopic" inhibition by sending wide, γ-aminobutyric acid (GABA)ergic axonal fields that densely ramify throughout the Ipc, SLu and the deep layers of TeO (Wang et al., 2004, 2006). Through this anatomical arrangement, visually activated tectal locations trigger feedback signals from corresponding loci in the Ipc and the SLu and at the same time, via Imc, can suppress tectal responses and their isthmic feedback at other tectal locations (Marín et al., 2007, 2012; Asadollahi et al., 2010; Mysore and Knudsen, 2013).

The feedback signals carried by Ipc axons are fast sequences of spike bursts that fire in synchrony with fast sequences of double or single spikes fired by SLu axons (Marín et al., 2012). Whereas the synaptic targets of Ipc and SLu axons remain undetermined, the bursting-firing of Ipc axons has a strong boosting effect on the ascending tectofugal transmission of retinal inputs, to the extent that the visual responses in the Rt and its pallial target, the entopallium, become synchronized to the rhythm of the feedback from the Ipc (Marín et al., 2012). Furthermore, preventing the feedback from the Ipc, but not from the SLu, in a tectal location, suppresses visual responses from the corresponding region of visual space in all Rt subdivisions. This led to the proposition that feedback from the Ipc exerts a focal effect, like an attentional "spotlight," on the bidimensional array of dendritic TGC terminals, enhancing the transmission of incoming visual flow from the optic tectum to higher visual areas (Wang et al., 2004, 2006; Marín et al., 2005, 2007, 2012).

Although it has been generally accepted that the Ipc and SLu axons are cholinergic (Wang et al., 2006; Maczko et al., 2006; Marín et al., 2007; Goddard et al., 2012, 2014) and that the strong control of the Ipc feedback on the TGC's output could be produced by presynaptic cholinergic modulation of the retinal inputs (Wang et al., 2006, Marín et al., 2012), the neurochemical identity of the Ipc nucleus is still unclear. Previous studies, based on uptake-and-release assays of radioactive molecules assigned a glycinergic and GABAergic identity to the Ipc neurons (Reubi and Cuénod, 1976; Hunt and Kunzle, 1976; Hunt et al., 1977), a conclusion supported by electrophysiological experiments showing that Ipc stimulation produced inhibitory effects in the tectum (Felix et al., 1994: Wang et al., 1995, 2000). In contrast, glutamate-like immunolabeling of presumptive Ipc axon terminals in the superficial tectal layers of pigeons suggested that the Ipc is glutamatergic (Morino et al., 1991). The issue was seemingly resolved by several studies using modern immunohistochemical techniques that show strong choline acetyltransferase (ChAT) immunoreactivity in both the Ipc and SLu of pigeons (Bagnoli et al., 1992; Medina and Reiner, 1994), chickens (Sorenson et al., 1989; Wang et al., 2006; our own results, Fig. 1), and barn owls (Mackzo et al., 2006). In the Ipc, ChAT expression included cell somas and their conspicuous axon terminals (Medina and Reiner, 1994), further supporting the cholinergic phenotype, which thenceforth became widely accepted. However, a subsequent study in pigeons showed a strong expression of vesicular glutamate transporter 2 (VGluT2) mRNA throughout the Ipc (Islam and Atoji, 2008).

The remarkable synchrony of the feedback signals provided by the Ipc and SLu, and the strong effect exerted by the Ipc feedback on tectofugal transmission, the physiological mechanism of which is presently unknown, underscores the importance of determining whether these coordinated signals are both cholinergic or involve different neurotransmitters. In this study we cloned specific cDNA sequences and synthesized RNA probes to perform in situ hybridization assays for VGluT2 and the three presynaptic cholinergic markers: the vesicular acetylcholine transporter (VAChT), the choline high-affinity transporter (CHT1), and the ChAT enzyme. The VAChT and VGluT2 proteins are considered critical neurochemical markers, as they transport the respective neurotransmitters into the synaptic vesicles (Liu et al., 1999; Fremau et al., 2004; El

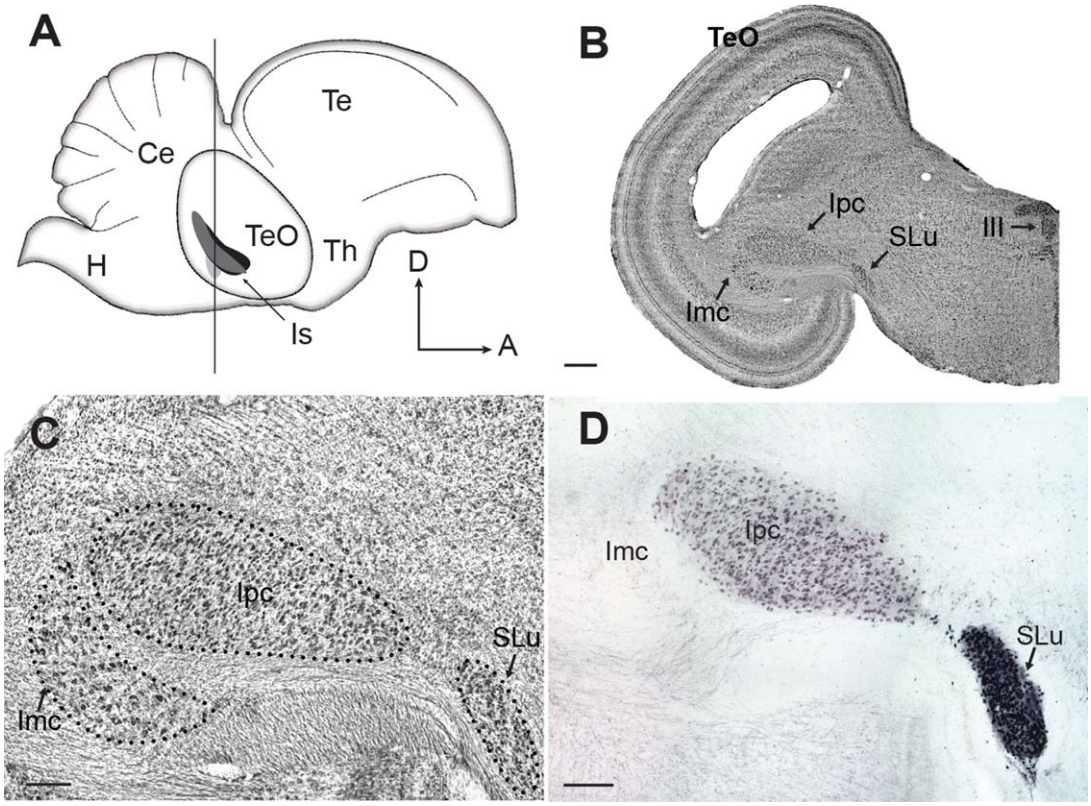

Figure 1. Isthmi pars parvocellularis (Ipc) and isthmi pars Semilunaris (SLu) choline acetyltransferase (ChAT) immunoreactivity. **A:** Schematic of a lateral view of the chicken brain displaying the location of the isthmic complex (Is). Ipc (black), SLu (ligth-grey) and Isthmi pars magnocellularis (grey). **B:** Microphotograph of a Nissl-stained coronal section at the midbrain level indicated by the vertical line in A. **C:** Enlarged view of B showing the isthmic complex. **D:** ChAT immunoreactivity within the isthmic complex. SLu neurons are strongly labeled in comparison with Ipc cells, which display moderately stained perikarya. No label is observed in the isthmi pars magnocellularis (Imc) neurons. III, oculomotor nucleus; TeO, optic tectum. Scale bar = 1 mm in B; 200 μm in C,D. [Color figure can be viewed in the online issue, which is available at wileyonlinelibrary.com.]

TABLE 1.

Sequences of PCR Primers Used to Amplify Specific cDNA Sequences of Each Marker

	Forward primer	Reverse primer	Annealing (°C)	Fragment (bp)
VAChT	5′-ATGTTCCTCTCCACCACCAC-3′	5Ç-CACGGCGATATAGGGGTCTA-3′	58.7	390
ChAT	5′-AGTGGGCAGAGGCCAGGACA-3′	5′-AGGATGCCAAGTGCGCCTGA-3′	62.0	414
CHT1	5′-TGCTGGCATCATCAGTGTACGGC-3′	5′-ACTGTACCTCGCAACCACAGCA-3′	62.0	379
VGluT2	5′-GGCTCTGCACGCCGTCTCTC-3′	5′-TCGATGGTGTCCCCGGGCTT-3′	61.5	317

Mestikawy et al., 2011). We also assayed VGluT2 protein expression in labeled Ipc axon terminals using neural tracing, immunohistochemical techniques, and confocal microscopy.

MATERIALS AND METHODS

Experiments were conducted on 37 broiler chickens (*Gallus gallus domesticus*; U.S. National Center for Biotechnology Information [NCBI] taxonomic ID: 9031) of both sexes, obtained from a local dealer and maintained in an institutional facility (in situ hybridization, $n = 31$; immunohistochemistry/immunofluorescence, $n = 4$; RNA and protein extraction, $n = 2$). The ages of the animals ranged from 1 to 40 days. All procedures were approved by the Ethics Committee of the Science Faculty of the University of Chile and conformed to the guidelines of the NIH on the use of animals in experimental research.

RNA probes and primers design

RNA probes were designed by using the chicken (*Gallus gallus*) nucleotide databases (NCBI Nucleotide, RRID:nlx_84100) and the alignment tools of the NCBI website (NCBI BLAST, RRID:nlx_84530; Primer-BLAST, RRID:OMICS_02343; http://www.ncbi.nlm.nih.gov). To amplify the cDNA corresponding to each probe, specific

pairs of primers (Table 1) were designed and commercially synthesized (IDT DNA, Coralville, IA). The selected transcript regions for each probe were the following: VAChT: NM_206982, 390 bp from nucleotides 433 to 822; ChAT: NM_204610, 414 bp from nucleotides 755 to 1,168; CHT1: NM_001001763, 379 bp from nucleotides 1,189 to 1,567; VGluT2: NM_001168383, 317 bp from nucleotides 14 to 330. Each chosen region was located in the coding region of its correspondent mRNA.

RNA extraction

Total RNA was isolated from mesencephalon of chickens ranging from 5 to 15 postnatal days. Brain tissue was homogenized in 1 ml of RNAsolv Reagent (Omega Bio-Tek, Norcross, GA) using a dounce homogenizer, mixed with 0.2 ml of chloroform, and vortexed for 15 seconds. The mixture was then incubated for 10 minutes on ice and centrifuged at 10,000 rpm for 10 minutes at room temperature (Eppendorf 5424 tabletop centrifuge). The aqueous phase was recovered, mixed with 0.5 ml of isopropyl alcohol, and incubated for 10 minutes prior to centrifugation at 10,000 rpm for 10 minutes at room temperature. The precipitated RNA pellet was washed with 1 ml of 80% ethanol, centrifuged at 8,500 rpm for 5 minutes at room temperature, air-dried, and reconstituted with 70 μl of nuclease-free water.

RT-PCR

Single-strand cDNA was synthesized by using Improm-II reverse transcriptase (RT; Improm-II™ Reverse transcriptase, Promega, Madison, WI) according to the manufacturer's instructions. Briefly, 1 μg of total RNA and 1 μl of oligo(dT) primer were incubated for 5 minutes at 70°C, and then a reverse-transcription cocktail cocktail was added (1 μl reverse transcriptase; 2.5 μl 25 mM $MgCl_2$; 1 μl RNAse inhibitor RNAsin, Promega; 1 μl 10 mM mixed DNTPs; 4 μl of 5X reaction buffer), and the mixture was incubated at 42°C for 60 minutes. The cDNA obtained served as a template for polymerase chain reaction (PCR) using Taq polymerase (Go-Taq, Promega). PCR protocols comprised 35 amplification cycles (denaturation 30 seconds at 94°C; annealing 60 seconds at temperature shown in Table 1; extension 50 seconds at 72°C; and finalized by a single 10-minute extension at 72°C). PCR products were analyzed in 1.5% agarose gels. Expected DNA fragments were excised from the gel and purified using a commercial kit (Wizard SV Gel and PCR clean-up system, Promega) according to the manufacturer's instructions.

Cloning

The four specific double-strand DNA sequences obtained were cloned into amplification vectors (pGEMT easy vector, Promega) according to the manufacturer's protocol. Heat-competent DH5α bacteria were transformed by thermal shock (42°C for 90 seconds) and seeded on Petri dishes with LB-Agar-XGal media (2.5% LB Broth, MO BIO, Carlsbad, CA; 2% Agar, Bacto Agar BD, Sparks, MD; 40 μg/ml XGAL, US Biological, Swampscott, MA). Positive clones (selected by blue/white screening) were amplified in liquid LB-ampicillin media (ampicillin, US Biological) at 37°C for 16 hours. Cells were pelleted by centrifugation (13,000 rpm) and plasmid DNA was purified by using a commercial miniprep kit (QIAprep spin miniprep kit, Qiagen, Valencia, CA). Purified DNA was commercially sequenced (Sequencing Service, P. Universidad Católica de Chile) and compared with published sequences.

RNA probes synthesis

To obtain template DNA for RNA probe synthesis, purified plasmid DNA was linearized by *Hin*cII or *Zra*I (Fermentas, Vilnius, Lithuania) restriction enzymes generating a sense or antisense template according to the orientation of the inserted fragment in the plasmid. For each probe, 5 μg of DNA were digested with 20 U of enzyme at 37°C for 16–20 hours in a final reaction volume of 100 μl. Linearized DNA was purified by using a commercial kit (Wizard SV Gel and PCR clean-up system, Promega) and used as template for RNA probe synthesis.

Digoxigenin-labeled RNA probes were synthesized in vitro by using SP6 and T7 RNA polymerases (Riboprobe in vitro transcription systems, Promega) and digoxigenin-labeled ribonucleotides (Dig RNA labeling mix 10X, Roche, Mannheim, Germany). The transcription mix (1 μg linearized DNA; 1 μl 100 mM dithiothreitol [DTT]; 1 μl RNasin; 1 μl 10 mM (each) ribonucleotides mix; 4 μl 5X transcription buffer; 1 μl SP6 or T7 enzyme) was incubated for 2 hours at 37°C. Finally, RNA digoxigenin probes were purified with a commercial kit (E.Z.N.A. RNA Probe purification kit, Omega Bio-Tek,) and stored at −80°C

In situ hybridization

Thirty-one chickens aged from 1 day to 4 weeks were perfused transcardially under deep anesthesia (ketamine 75 mg/kg, xylazine 5 mg/kg) using 300 ml of saline solution (NaCl 0.75%) followed by 250 ml of fixative (0.01 M phosphate buffer pH 7.4; 0.75% NaCl; 4% paraformaldehyde [PFA]). Brains were removed and incubated in cryoprotective/postfixative solution (30% sucrose; 4% PFA in diethylpyrocarbonate [DEPC]-treated water) for 24–48 hours at 4°C. Once the brains had sunk, they were mounted on a freezing sliding microtome (Leitz 1400) and cut in coronal sections of 80–

TABLE 2.
Primary Antibodies Used

Antigen	Immunogen	Source, host species, cat. #, clone or Lot #, RRID	Concentration
Digoxigenin	Digoxigenin	Roche Diagnostics, anti-digoxigenin-AP Fab fragments, RRID:AB_514497	1:1,000
Choline acetyltransferase (ChAT)	Human placental ChAT	Millipore, goat anti-ChAT, cat. #AB144P-200UL, RRID:AB_90661	1:2,000
Phaseolus vulgaris leucoagglutinin (PHA-L)	Pure lectins	Vector, unconjugated, rabbit anti-PHA-L, cat. #2300, RRID:AB_2315140	1:5,000
Vesicular glutamate transporter 2 (VGluT2)	Fusion protein amino acids 501–582 (cytoplasmic C-terminus) of rat VGlut2	NeuroMab, mouse anti-VGluT2 N29/29, cat. #75-067, RRID:AB_2239153	1:2,000

100 μm. Free-floating sections were washed three times in phosphate-buffered saline (PBS; 0.01 M phosphate buffer pH 7.4; 0.02% NaCl in DEPC-treated water) and treated with peroxide/PBS-T solution for 30 minutes (6% hydrogen peroxide; 0.1% Tween-20; Promega). The sections were then incubated in proteinase K/PBST solution (Proteinase K 10 μg/ml, Promega) for 10 minutes at room temperature (after different incubation times were tested for optimal permabilization), washed once in PBST, fixed in 4% PFA/PBST for 20 minutes, washed three times in PBST, and prehybridized at 65°C in hybridization buffer for 3 hours (50% formamide, Merck, Darmstadt, Germany; 1.3X standard saline citrate [SSC], pH 5.3, Winkler, Santiago, Chile; 5 mM EDTA, Winkler; 200 μg/ml tRNA from salmon sperm; 0.002% Tween-20; 0.005% CHAPS, Calbiochem, La Jolla, CA; 100 μg/ml heparin, Calbiochem).

After addition of the specific RNA probes and incubation for 16–18 hours at 65–70°C, the sections were washed twice in solution A (5X SSC, pH 5.3; 50% formamide; 1% sodium dodecyl sulfate [SDS]) at 65°C for 30 minutes and three times in solution B (2.5X SSC, pH 5.3; 50% formamide; 1% Tween-20) at 65°C for 30 minutes. After two washes in maleic acid buffer solution (MABT; 100 mM maleic acid, Sigma, St. Louis, MO; 150 mM NaCl; 0.1% Tween-20), the sections were incubated in blocking solution (2% Blocking Reagent, Roche, Indianapolis, IN; 2% heat-inactivated normal goat serum, in MABT) for 4 hours at room temperature and then incubated for 16–20 hours at 4°C with anti-digoxigenin-AP Fab fragments (1:1,000 dilution in MABT; Roche Diagnostics; RRID:AB_514497; Table 2). Finally, the sections were washed six times in MABT, incubated in alkaline reaction buffer (100 mM Tris, pH 9.5; 50 mM $MgCl_2$; 100 mM NaCl; 1% Tween-20), and developed at room temperature by adding NBT/BCIP reagent (NBT 375 μg/ml; BCIP 188 μg/ml; Stock Solution, Roche, Mannheim, Germany).

Surgical procedures for tracer injections

Chickens were anesthetized by an intramuscular injection of ketamine (75 mg/kg) and xylazine (5 mg/kg) and placed in a stereotaxic frame. Anesthesia was maintained during surgery and throughout the experiment by infusing 15% of the initial dose every 90 minutes via an intramuscular cannula. Body temperature of the animal was maintained between 40 and 42°C by a thermoregulated blanket (DC temperature controller; FHC, Bowdoin, ME). A small window was opened in the right side of the skull exposing the dorsolateral part of the tectum, and the overlying dura was punctured by using a fine forceps.

Phaseolus vulgaris leucoagglutinin injections

To assess the colocalization of VGluT2 reaction granules with the Ipc axonal branches, five animals received an injection of the anterograde tracer *Phaseolus vulgaris* leucoagglutinin PHA-L (Vector, Burlingame, CA) in the Ipc. In three of these animals, the eye contralateral to the injection was removed, to induce degeneration of the retinal terminals in the TeO. To locate the Ipc nucleus, exploratory stereotaxic recordings were performed by using tungsten electrodes (1 MΩ, FHC) and an extracellular amplifier (model 3600, AM Systems, Sequim, WA). Bursting responses to visual motion, characteristic of Ipc neurons (Marín et al., 2005), were elicited by using a hand-held laser beam moved on a tangential screen. Once identified, a PHA-L–filled micropipette (2.5% PHA-L in 10 mM phosphate buffer, pH 8) with a 10–15-μm tip diameter was lowered, and the Ipc nucleus was iontophoretically injected (7 μA for 35 minutes with a 7-second on, 7-second off cycle). Animals were perfused after 7 to 10 days (nonenucleated) and 30 days (enucleated).

Immunohistochemistry and immunofluorescence

After perfusion, the brains were removed and incubated in cryoprotective/postfixative solution (30%

sucrose; 4% PFA) for 24–48 hours, and 60-μm coronal sections were cut by using a freezing microtome (Leitz 1400). Sections were washed three times in 0.01 M PBS, incubated in a citrate buffer solution (0.01 M sodium citrate, pH 6.0) at 80°C for 30 minutes, washed three times in PBS, and incubated for 60 minutes in normal donkey serum blocking solution (NDS/PBST; 0.01 M phosphate buffer, pH 7.4; 3% NDS; 0.1% Triton X-100; Promega). Primary antibodies were added, and sections were incubated for 24 hours at 4°C. Anti-PHA-L primary antibody (unconjugated rabbit anti-PHA-L, Vector cat. #2300, RRID:AB_2315140; Table 2) was used at a dilution of 1:5,000 in 3% NDS-PBST; the anti-VGluT2 primary antibody (mouse anti-VGluT2 N29/29, NeuroMab, Davis, CA, cat. #75-067, RRID:AB_2239153; Table 2) was used at a dilution of 1:2,000 in 3% NDS-PBST; and anti-ChAT primary antibody (goat anti-ChAT, Millipore, Temecular, CA, cat. #AB144P-200UL, RRID:AB_90661; Table 2) was used at a dilution of 1:2,000 in 3% NDS/PBST.

For single immunolabeling of VGluT2 and ChAT, primary antibody incubation was followed by three washes with PBS and 2 hours of incubation with anti-mouse (Vector, cat. #BA2000, RRID:AB_2313581) or anti-goat (Vector, cat. #3BA-5000, RRID:AB_2336126) biotinylated secondary antibodies at a dilution of 1:200 in 3% NDS/PBST. After three washes with PBS, avidin–biotin–peroxidase complex (ABC; Vector) was added, and the sections were incubated on a shaker for 1 hour at room temperature followed by three washes in PBS and one in Tris buffer (0.05 M Tris, pH 7.4). The sections were developed for 10 minutes in DAB solution 3,3′-diaminobenzidine tetrahydrochloride (DAB) solution (0.025% in Tris buffer, Sigma) and 0.01 M nickel sulfate (Merck). Following addition of H_2O_2 solution (0.03%, final concentration), the reaction was continued for 3–5 minutes until labeling was clearly observed. The reaction was stopped by adding Tris buffer. After two washes in PBS, the sections were washed once in 0.1 M phosphate buffer (PB; pH 7.4). For single immunolabeling of PHA-L injections, after the biotinylated primary incubation, the sections were washed three times in PBS and directly incubated in an ABC solution and revealed as described above.

For double immunofluorescence, the primary antibodies, rabbit anti-PHA-L, and mouse anti-VGluT2 were added together at the incubation step. The sections were then washed three times in PBS and incubated with complementary fluorescent secondary antibodies (Alexa Fluor 568 goat anti-mouse IgG (H+L), Life Technologies, Bethesday, MD, cat. #A11031, RRID:AB_10562420; Alexa Fluor 488 goat anti rabbit IgG (H+L), Life Technologies, cat. #A11034, RRID: AB_10562715).

Antibody characterization

See Table 2 for a list of all antibodies used. The unconjugated anti–PHA-L antibody strongly reacts with PHA-L injected locally in neural tissue; uninjected tissue exhibits no anti-PHA-L reactivity. The anti-ChAT antibody reacted as expected (data not shown) with all known cholinergic structures in the avian brain (Sorenson et al., 1989; Medina and Reiner, 1994). The anti-VGluT2 antibody was characterized by immunoblot of chicken whole brain proteins. Immunoblot analysis showed a single 65-kDa VGluT2-immunoreactive band (data not shown). This is in agreement with the molecular weight estimation for the chicken VGluT2 (585 amino acids; 64.6 kDa; accession number: NP_001161855.1).

Cell density estimation

To assess whether VGluT2 in situ hybridization and ChAT immunoreactivity labeled all lpc neurons, the density of labeled neurons obtained in each condition was estimated and compared with that obtained in Nissl-stained material. Two 8-week-old chickens were perfused, and the brains removed, incubated in cryoprotective/postfixative solution (30% sucrose; 4% PFA) for 24–48 hours, and cut into 80-μm coronal sections using a freezing microtome (Leitz 1400); three series were obtained from each brain. In both brains, the respective series were used for VGluT2 in situ hybridization, anti-ChAT immunohistochemistry, and Nissl staining. By using the optical fractionator method in the MBF Stereo Investigator software (MBF Bioscience, Williston, VT) we counted lpc cells in five alternate sections from each series. In each section, a counting frame of 80 × 80 μm was used, with a depth in the z-axis of 20 μm. The grids were place over the lpc by using a Systematic Random Sampling grid. Section thickness was measured at each position by using the microscope focus. Guard zones were established above and below the z-limits of the counting frame. As each staining or labeled method displays different labeling features (e.g., the nucleolus is visible in the Nissl staining, but is absent in the immunostained and in situ preparations), we used a common criterion to select the neurons to be counted in each of the series. Neurons were counted when their largest diameter came into focus inside the counting box (thus those cells were not selected that "touched" an exclusion plane located at the top of the counting box), while also not touching any of the lateral exclusion planes (located in two contiguous sides of the counting box) (Gundersen et al., 1988). To estimate the cellular density, the total number of counted cells was divided by the total sampling volume. For every treatment the volume was

corrected for tissue compression (z-axis), calculated by dividing the cutting section thickness by the mean thickness value measured in each mounted sections. This value was multiplied by the total counting volume to obtain the corrected total sampling volume. The informed cell density values are the mean obtained in both animals.

RESULTS

In situ hybridization

In situ hybridization assays for VAChT ($n = 13$), ChAT ($n = 6$), CHT1 ($n = 6$), and VGluT2 ($n = 6$) were performed in coronal brain sections of chickens ranging from 1 to 40 days old (p1–p40). Because no differences were observed across this age range, the data are presented as a single group. All antisense probes used gave distinct and specific labeling, according to the assayed brain region, and the results were highly repeatable across different animals. Furthermore, no labeling was detected when the sense probes were used.

Isthmic complex

As expected from the cholinergic identity suggested by ChAT immunohistochemistry (Sorenson et al., 1989; Medina and Reiner, 1994; Wang et al., 2006), the three cholinergic markers were strongly expressed in the SLu neurons (Fig. 2; VAChT, ChAT, and CHT1 panels). The intensity of labeling for these neurons was similar to that displayed by cholinergic neurons within the oculomotor complex and the other motor nuclei of the brainstem. Labeled neurons were densely packed, as SLu neurons normally look in Nissl-stained sections, indicating that all neurons within the nucleus had been labeled. Surprisingly, no VAChT mRNA expression was observed within the Ipc nucleus, which only showed weak ChAT and moderate CHT1 labeling (Fig. 2). The lack of VAChT expression was very consistent and occurred under several incubation protocols (including different hybridization temperatures and permeabilization conditions; see Materials and Methods), all of which resulted in intense labeling in the SLu and the cholinergic motor nuclei. In contrast, Ipc cells consistently showed a very intense VGluT2 mRNA expression (Fig. 2), which appeared to encompass all the neuronal somata of this nucleus. This was confirmed by comparing the density of VGluT2-labeled neurons (9.03×10^3 cells/mm^3, SD $= 4.04 \times 10^2$; $n = 2$) with the density estimated in Nissl-stained sections (1.08×10^4 cells/mm^3, SD $= 4.27 \times 10^2$; $n = 2$) in the Ipc. A similar cell density was obtained for ChAT immunostained neurons (9.22×10^3 cells/mm^3, SD $= 2.14 \times 10^3$; $n = 2$), indicating that all neurons in the Ipc contain VGluT2 mRNA and are also ChAT immunopositive.

In contrast, as expected from its GABAergic identity (Domenici et al., 1988; Wang et al., 2004; Sun et al., 2005), the Imc nucleus was unlabeled in all the in situ hybridization assays using either the cholinergic or the glutamatergic probes (Fig. 2).

Taken together, these results suggest that, in the chick, Ipc neurons are glutamatergic and that the expression of the cholinergic phenotype is incomplete. The cholinergic identity of the SLu nucleus is strongly supported.

Other brain structures

The three cholinergic markers and the glutamatergic marker consistently labeled all the known cholinergic and glutamatergic structures in the chicken brain. Only a few discrepancies were found, like the nucleus spiriformis medialis (SpM). A detailed description of labeling throughout the various regions of the chicken brain follows.

Medulla and pons

VAChT, ChAT, and CHT1 mRNAs were strongly expressed in all the neurons belonging to the motor nuclei of the pons and medulla, including the trigeminal motor nuclei (Vmv, Vmd; Fig. 3A), the abducens (VIm), the facial nuclei (VIIv, Fig. 3A; VIId), the nucleus ambiguus (Amb), the dorsal nucleus of the vagus nerve (Xm), and the hypoglossal nucleus (XIIm). Intense labeling was also observed in some neurons of the locus coeruleus (LoC), the mediodorsal tegmental nucleus (MDT), and the laterodorsal tegmental nucleus (LDT), and in scattered neurons around the cochlear nucleus. High levels of VGluT2 expression were observed in the medial (PM) and lateral pontine nuclei (PL), gigantocellular reticular nucleus (Rgc), principal sensory trigeminal nucleus (PrV), and raphe nucleus (R). The auditory nuclei magnocellularis (NM), anterior (NA), and laminaris (NL) were also VGluT2 mRNA positive. In the cerebellum, the granular layer and cerebellar nuclei (Cbl, CbM) were VGluT2 mRNA positive (Fig. 3A), as were neurons in all vestibular nuclei (VS, VeM, VeL).

Mesencephalon

All divisions of the oculomotor nucleus, the Edinger–Westphal (EW) nucleus, the trochlear (IV) nucleus, and the tegmental cholinergic cells of the pedunculopontine tegmental nucleus (PPT) showed strong expression of the three cholinergic probes (Fig. 2). Neurons in tectal layer 10 exhibited barely detectable levels of ChAT mRNA expression; indeed, faint staining was only observed in a few experiments.

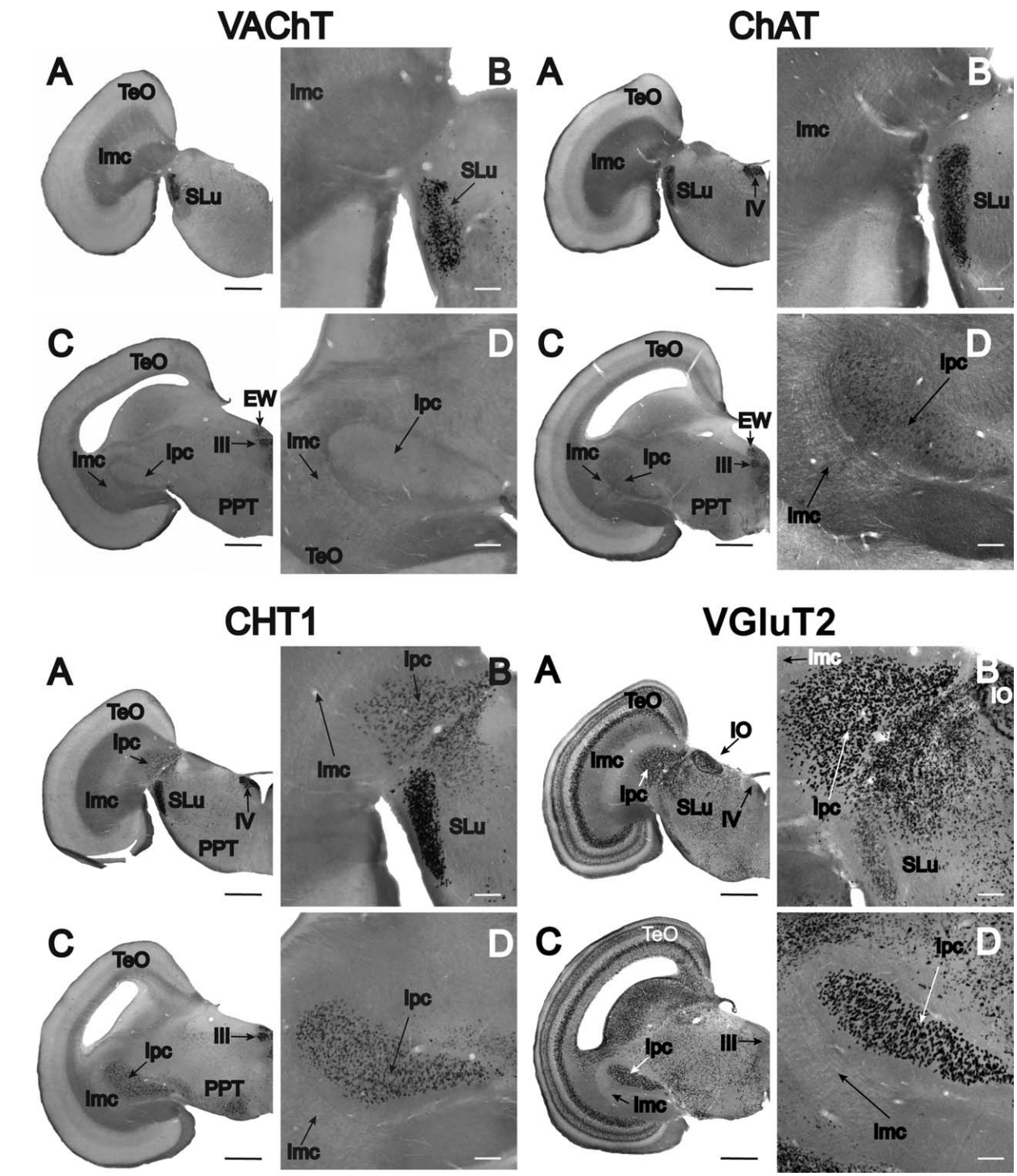

Figure 2. Expression of cholinergic and glutamatergic markers in the Ipc and SLu nuclei. Coronal sections of the isthmi and mesencephalon (**A** and **C** for all four markers) showing in situ hybridizations for the vesicular acetylcholine transporter (VAChT), choline acetyltransferase (ChAT), the choline high-affinity transporter (CHT1), and the vesicular glutamate transporter 2 (VGluT2) mRNAs. The mRNAs for the three cholinergic markers are strongly expressed in the SLu nucleus. The Ipc nucleus moderately expresses the CHT1 mRNA and lightly expresses the ChAT mRNA, whereas VAChT labeling is absent. In contrast, VGluT2 mRNA is strongly expressed in the Ipc and weakly in the SLu. Note that in all cases the GABAergic nucleus Imc shows no label. **B,D:** Enlarged views of A and C. All images displayed correspond to simultaneously treated series (one for each marker) obtained from a single brain. EW, Edinger–Westphal nucleus; IO, isthmo-optic nucleus; IV, trochlear nucleus; PPT, pedunculopontine tegmental nucleus. For other abbreviations, see Figure 1 legend. Scale bar = 1 mm in A,C; 200 μm in B,D.

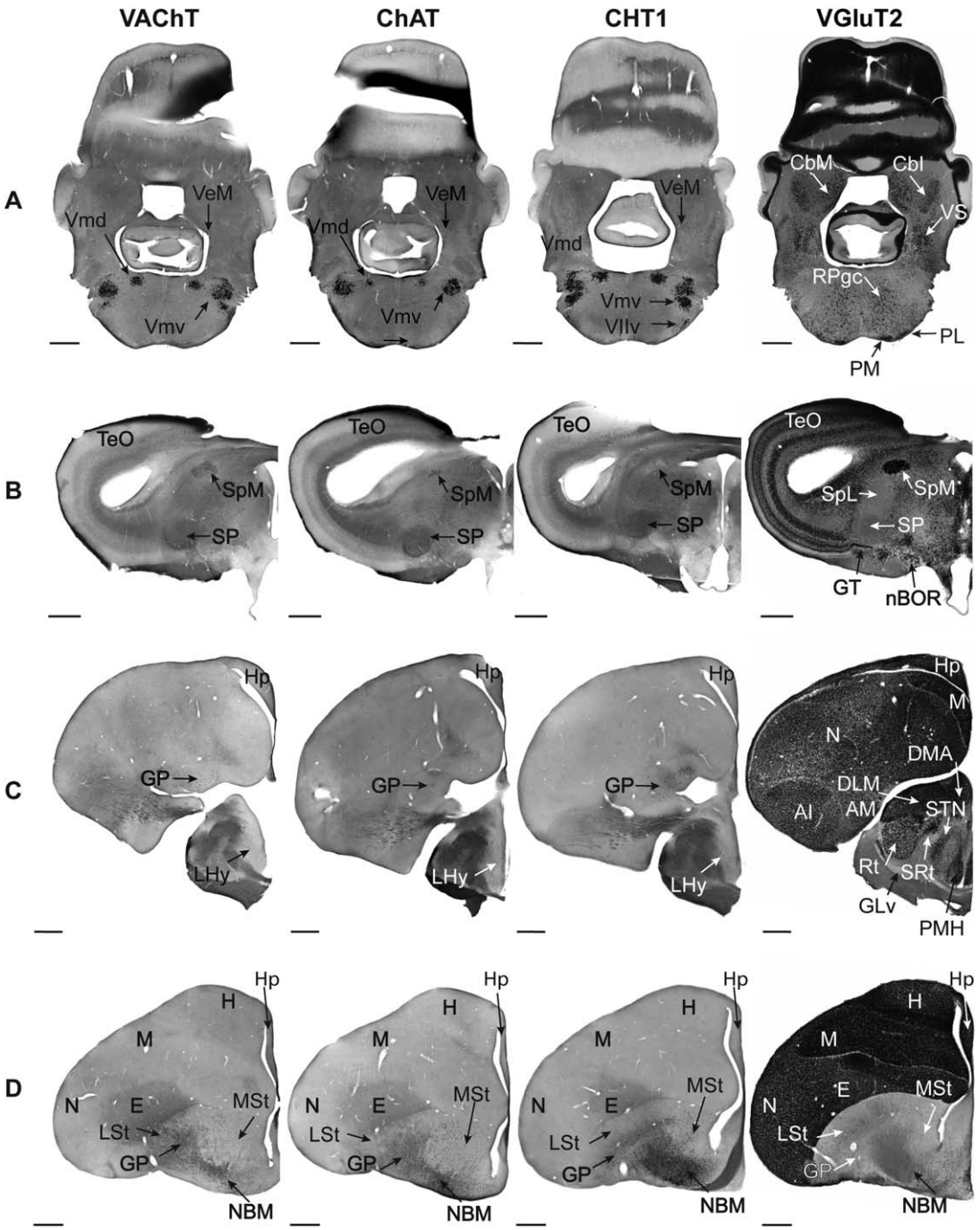

Figure 3. Cholinergic and glutamatergic marker expression in the principal areas of the chicken brain. **A:** Rhombencephalon. **B:** Pretectum. **C:** Diencephalon. **D:** Telencephalon. All images displayed correspond to simultaneously treated series (one for each marker) obtained from a single brain. AI, intermediate arcopallium; AM, anterior arcopallium; CbM, medial cerebellar nucleus; CbI, internal cerebellar nucleus; DLM, thalamic medial dorsolateral nucleus; DMA, thalamic anterior dorsomedial nucleus; E, entopallium; GLv, lateral geniculate nucleus pars ventralis; GP, globus pallidus; H, hyperpallium; Hp, hippocampus; LHy, lateral hypothalamic area; LSt, lateral striatum; M, mesopallium; MSt, medial striatum; N, nidopallium; NBM, basal magnocellular cholinergic nucleus; PM, medial pontine nucleus; PMH, posteromedial hypothalamic nucleus; PL, lateral pontine nucleus; RPgc, gigantocellular caudal pontine reticular nucleus; Rt, nucleus rotundus; SP, subpretectal nucleus; SpL, lateral spiriform nucleus; SpM, medial spiriform nucleus; SRt, nucleus subrotundus; STN, subthalamis nucleus; VIIv, facial motor nucleus pars ventralis; Vmd, trigeminal nucleus pars dorsalis; Vmv, trigeminal nucleus pars ventralis; VS, superior vestibular nucleus. Scale bar = 1 mm in A–D.

VGluT2 mRNA expression was very strong in the dorsal part of the lateral mesencephalic nucleus (MLd), and in the nucleus intercollicularis (ICo), lateral lemniscal nucleus, pars dorsalis (LLd), and isthmo-optic nucleus (IO). Scattered neurons were also labeled within the ventral tegmental area (VTA). In the tectum, intense labeling was found in layers 4, 6, 8, 9, 10, 11, 13, and 14 (Fig. 2) and in the stratum griseum periventriculare (SGPv).

Pretectum

The nucleus spiriformis medialis (SpM) showed clear expression of VAChT and ChAT mRNAs but not CHT1 mRNA (Fig. 3B). High levels of VGluT2 expression were also detected within this nucleus. Double in situ assays must be carried out to determine whether they correspond to the same or different neural populations. Other nuclei displaying intense VGluT2 staining were the nucleus of the basal optic root (nBOR) and the tectal gray nucleus (GT). The lateral spiriform nucleus (SpL) and subpretectal nucleus (SP), both considered GABAergic (Domenici et al., 1988; Veenman and Reiner, 1994; Sun et al., 2005), were devoid of any staining (Fig. 3B).

Diencephalon

Dispersed neurons in the nucleus lateralis hypothalamic (LHy) showed faint VAChT and ChAT expression and a moderate CHT1 expression (Fig. 3C). Neurons within the caudal part of the medial habenula (HM) were found to be weakly labeled for VAChT, ChAT, and CHT1 mRNAs. High levels of VGluT2 expression were found within the nucleus rotundus (Rt), nucleus subrotundus (SRt) (Fig. 3C), nucleus triangularis (T), subthalamic nucleus (STN), nucleus ovoidalis (Ov), medial habenula, and dorsolateral posterior nucleus (DLP). Moderate expression was observed in the nucleus dorsolateralis anterior thalami pars magnocellularis (DLAmc), the nuclei dorsolateralis anterior thalami pars medialis (DLM; Fig. 3C) and lateralis (DLL), the nucleus dorsomedialis anterior thalami (DMA; Fig. 3C), the posterior thalamis nucleus (DMP), the lentiformis mesencephali complex, and the nucleus principalis precommissuralis (PPC). The hypothalamus, nucleus medialis (PMH) (Fig. 3C), and lateralis (PLH) hypothalamic posterioris were also VGluT2 positive.

Telencephalon

All three cholinergic markers were strongly expressed in scattered neurons throughout the globus pallidus (GP), the nucleus basalis magnocellularis (NBM), and the medial striatum (MSt) (Fig. 3D). VGluT2 expression was high in most pallial structures, including the hippocampus (Hp), the mesopallium (M), and the hyperpallium (H), particularly the dorsal (HD) and the intercalated (HI) layers. Conspicuous primary sensory structures like the entopallium (E), the nucleus basalis (Bas), field L (L1, L2, L3), and all subdivisions of the arcopallium (A) were clearly labeled. Dispersed cells in the striatum (MSt; LSt) and the globus pallidus (GP), were also VGluT2 positive (Fig. 3D). The NBM was devoid of VGluT2 staining (Fig. 3D).

VGluT2 immunoreactivity

The mRNA expression profile described above strongly suggests a glutamatergic identity for the Ipc, because its neurons would be able to pack glutamate into their presynaptic vesicles. Nevertheless, the VGluT2 mRNA expression in Ipc neuronal somas does not necessarily imply that the VGluT2 protein is deployed in the axon terminals. Therefore, we performed double immunostaining assays in which the Ipc was filled anterogradely with the neural tracer PHA-L, and the presence of the VGluT2 protein was determined by both DAB immunoprecipitation and immunofluorescence. Because there is no commercial antibody against chick VGluT2, we used a commercially available monoclonal antibody produced against the rat VGluT2 protein c-terminal sequence (accession number: NP_445879.1, amino acids 501–582). This immunogenic peptide shares a high amino acid sequence identity (84%) with the chicken VGluT2 protein c-terminal sequence (accession number: NP_001161855.1). The molecular weight estimation for the chicken VGluT2, 585-amino acid sequence, is 64.6 kDa (accession number: NP_001161855.1), which agrees with the VGluT2-immunoreactive 65-kDa single band obtained by our own western blot analysis (data not shown).

In general, VGluT2 immunoreactivity across the chicken brain was consistent with the distribution described for pigeons, using a different antibody (Atoji, 2011). In the tectum, VGluT2 immunoreactivity was observed as fine granules and varicosities, which were especially dense in the retino-recipient layers (layers 2–7; Fig. 4B). Moderate labeling was also evident in tcellular layers 10 and 13. Because the Ipc axonal terminals colocalize in the superficial tectal layers with the glutamatergic retinal terminals, especially in layer 5, it was difficult to determine their respective contribution in the VGluT2-immunopositive profile. However, the structure of the immunoreactive granules in the superficial layers looked similar to the pattern of labeled Ipc axon terminals seen in ChAT-immunoreactive sections. Three chickens were enucleated to eliminate the contribution of the retinal ganglion cells terminals, and their brains were examined for VGluT2 immunoreactivity after 30

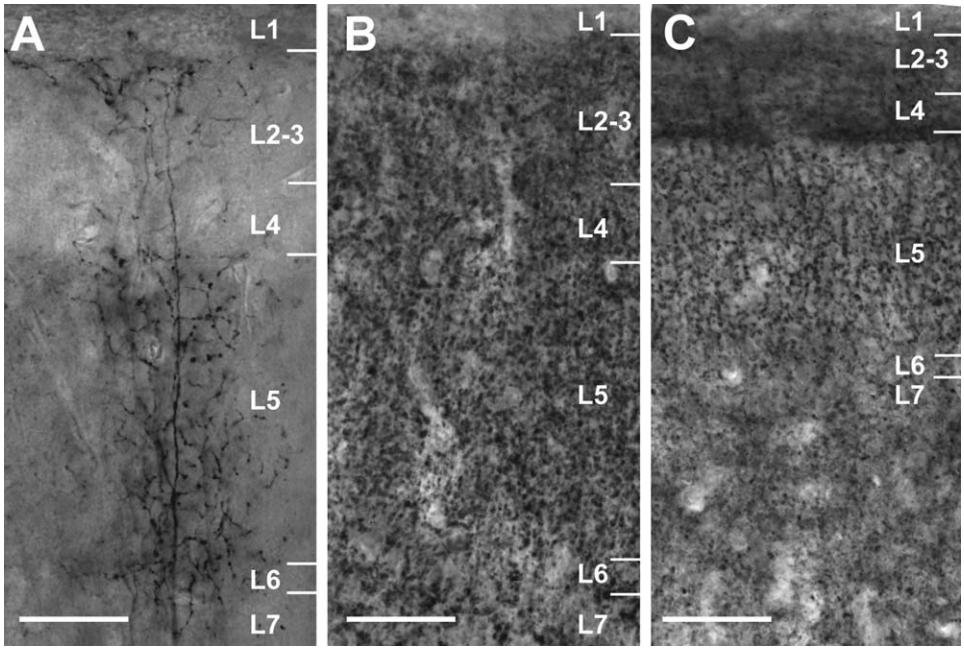

Figure 4. VGluT2 immunohistochemistry in the superficial layers of TeO in normal and enucleated chicks. Each panel shows a low-power photomicrograph of the tectal retinorecipient layers. **A:** A PHA-L–filled Ipc paintbrush axon terminal showing the dense distribution of terminal branches and synaptic boutons from layers 2 (L2) to 5 (L5). **B:** VGluT2 immunoreactivity in an equivalent section. Note the dense immunopositive granules in tectal layers 2 to 7 (L7), presumably corresponding to retinal terminals and Ipc axons boutons. **C:** VGluT2 immunoreactivity in an enucleated chick (30-day survival time). In the shrunk superficial layers devoid of retinal terminals, the less dense granules are more conspicuous and resemble Ipc axon terminals. Scale bar = 50 μm in A–C.

days, a period that allows for complete degeneration of the retinal terminals in the tectum (Gray and Hamlyn, 1962; Cuénod et al., 1970; Hayes and Webster, 1975; Hunt and Webster, 1975; Reperant and Angaut, 1977). As shown in Figure 4C, the shrunk retino-recipient tectal layers of an enucleated chicken still show granular VGluT2 immunoreactivity, which is especially evident in layer 5.

In the same enucleated animals, we assessed the colocalization of VGluT2 and PHA-L immunofluorescence in the PHA-L–filled axon terminals. Fluorescent-labeled VGluT2-immunoreactive granules closely coincided with the fine structure of the boutons and varicosities of the Ipc axon terminal arborizations (Fig. 5, upper and central row). Confocal imaging of similar material demonstrates the clear overlap between VGluT2 immunoreactivity and the Ipc terminal boutons, indicating that Ipc neurons express the VGluT2 protein in their axons (Fig. 5, lower row).

DISCUSSION

The present results on chickens suggest the necessity to re-examine assumptions regarding the purely cholinergic nature of the isthmic nuclei homotopically connected to the TeO. The glutamatergic identity proposed for the Ipc implies that the homotopic feedback mediated by the Ipc and SLu is more heterogeneous than previously assumed. This is particularly interesting considering that these homotopic feedbacks are simultaneous and synchronized and appear to affect an entire tectal column. The Ipc feedback boosts the propagation of the retinal inputs from the tectum to higher visual areas (Marín et al., 2007, 2012), a function that may depend more heavily on the synaptic release of glutamate than of acetylcholine.

Neurochemical identities of the Ipc and SLu

The Ipc and SLu establish two parallel and homotopic feedback projections to the TeO, which up to now were both considered cholinergic. This study supports the cholinergic function of the SLu neurons, as these were the only neurons expressing, at the mRNA level, the three cholinergic markers, VAChT, ChAT, and CHT1. Instead, the Ipc nucleus, largely accepted as purely cholinergic due to its ChAT immunoreactivity (Sorenson et al., 1989; Bagnoli et al., 1992; Medina and Reiner, 1994), did not show detectable levels of VAChT mRNA, even though its neurons showed ChAT and CHT1 mRNA expression, albeit at a weaker level than the neurons in the SLu. According to these results, Ipc neurons could

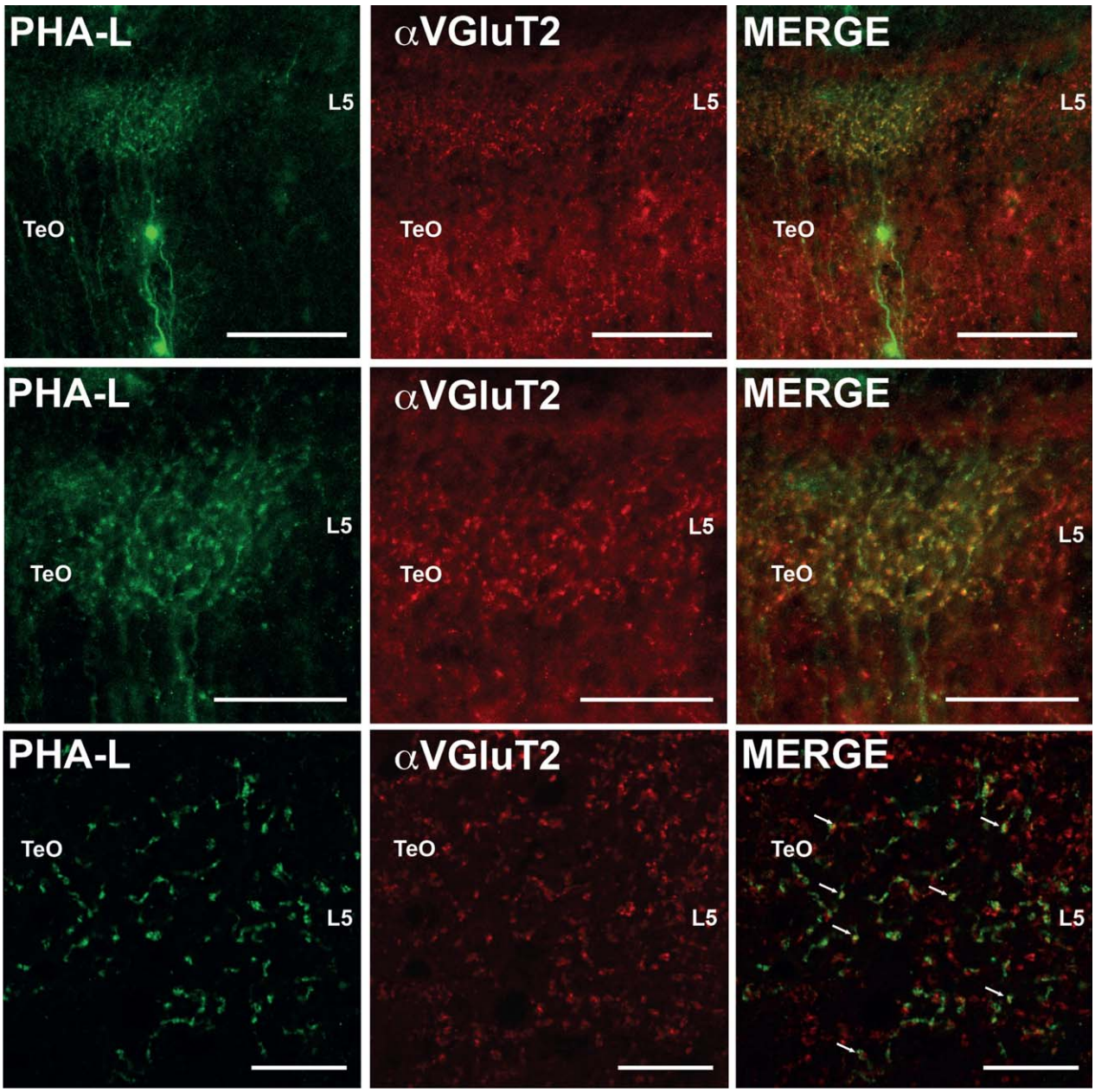

Figure 5. VGluT2 coexpression in PHA-L–labeled Ipc axon terminals in enucleated chickens. **Top row:** Low-power epifluorescent microphotographs of the superficial layers of TeO from a double immunofluorescence experiment showing a PHA-L–filled Ipc axon (green fluorescence, Alexa 488; left), the corresponding anti-VGluT2 immunoreactivity (red fluorescence, Alexa 568; middle), and the superimposed label. **Middle row:** Same as above at higher magnification. **Bottom row:** High-power confocal imaging from a similar experiment in a different animal showing the codistribution of PHA-L–filled boutons and VGluT2 immunoreactivity. TeO, optic tectum. Scale bar = 150 μm in upper row; = 75 μm in middle row; 20 μm in bottom row.

uptake choline molecules from the extracellular space and synthesize acetylcholine, but the neurotransmitter packing into synaptic vesicles, a critical last step for vesicular release, would be weakened.

Absence of VAChT mRNA expression was restricted to the Ipc, and was consistent throughout the assays ($n = 13$), whereas the other nuclei in the brain considered cholinergic were strongly labeled. A specific resistance of the Ipc to probe penetrability cannot explain these results, as the other three probes did label the Ipc under identical methodological conditions. Apart from the Ipc, the three cholinergic markers were codetected in most cholinergic nuclei, with the exception of the SpM, where VAChT and ChAT are expressed but CHT1 mRNA was not detected. The cholinergic probes were also very specific, as there were no labeled

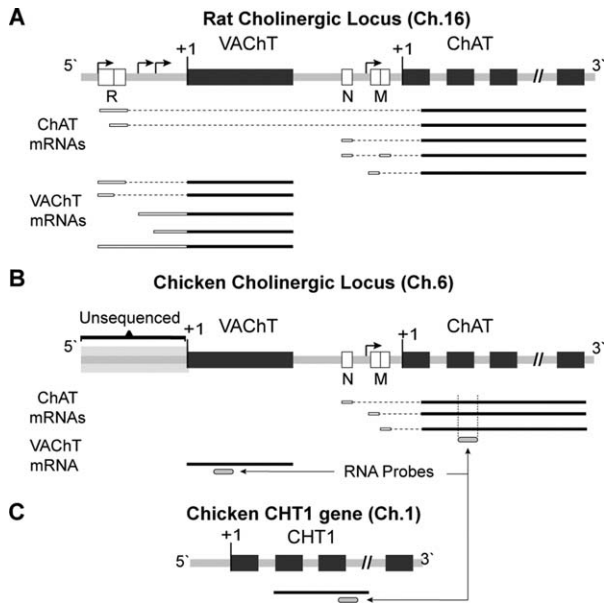

Figure 6. The cholinergic locus. **A,B:** Schematic representation of the rat and chicken cholinergic locus. The black and white boxes indicate coding and noncoding transcribed sequences (exons), respectively. Arrows indicate the transcriptional start sites for both VAChT and ChAT genes. **A:** In the rat, the VAChT and ChAT genes possess shared (R region) and exclusive (arrows) start sites, which lead to the expression of different 5′ untranslated regions (5′-UTR) mRNA species. **B:** The chicken cholinergic locus is partially sequenced, and few mRNAs species of each protein have been identified. To cover every possible VAChT and ChAT isoforms, both VAChT and ChAT digoxigenin-labeled RNA antisense probes were directed to coding regions of each correspondent transcript. **C:** The gene coding for the CHT1 is located in a different chromosome than the cholinergic locus. The RNA antisense probe for this marker was directed to a coding region of the transcript. Ch.1, chromosome 1; Ch.6, chromosome 6; Ch.16, chromosome 16; +1, translation initiation codon.

profiles in nuclei or areas that have been described as noncholinergic.

Whether or not other VAChT transcripts may exist in the chicken brain that were not detected by our probe, it has been shown in the chicken (Mukherjee and Hausman, 2004), as well as in other vertebrates (Bejanin et al., 1994; Roghani et al., 1994; Naciff et al., 1997), that the cholinergic locus contains both the VAChT and ChAT genes, where the VAChT gene is a single uninterrupted coding region with no introns, nested in the first intron of the ChAT gene (Fig. 6). Several 5′ untranslated regions (UTRs) mRNA isoforms of the VAChT gene have been described in mammals (Roghani et al., 1994; Bejanin et al., 1994; Cervini et al., 1995; Erickson et al., 1994). Therefore, the VAChT gene structure makes alternative-splicing variants of the VAChT unlikely. Although UTR VAChT transcript isoforms in the chicken are unknown, our probe was directed to a large 390-bp segment of the transporter transcript, which codes for the trans-membrane domains 3–7 of the VAChT protein, located in the invariable coding region of all the VAChT isoforms in mammals. Thus our probe should recognize equivalent transcription variants that could occur in the chick.

A possible downregulation of the cholinergic locus in the lpc neurons

The diminished expression of VAChT mRNA in the lpc, along with a mild expression of the ChAT mRNA and protein, suggests a partial downregulation of the cholinergic locus. Detailed studies in the rat (Bejanin et al., 1994; Roghani et al., 1994; Cervini et al., 1995; Mallet et al., 1998) (Fig. 6A) show that VAChT and ChAT share a start site (the R region) that produces a primary transcript spanning the entire locus, which by alternative splicing could originate the ChAT and VAChT mature mRNAs (Fig. 6, R region). In contrast, there are exclusive VAChT- and ChAT-promoting sequences expressing several 5′UTR variants that can be coexpressed or regulated individually (Bejanin et al., 1994; Erickson et al., 1994; Berrard et al., 1995; Cervini et al., 1995; Mallet et al., 1998; Shimojo et al., 1998; Weihe et al., 1998; Schütz et al., 2001; Castell et al., 2002, 2003; Brock et al., 2007). Currently, all evidence indicates that this independent control of each gene predominates in the rat, and that the coupled expression directed by the R start site is less significant (Schütz et al., 2001). In chickens, the N- and M-type ChAT noncoding exons have been detected, but the upstream region of the VAChT gene containing the R region has not been sequenced (Mukherjee and Hausman, 2004). Only the N-type ChAT mRNA isoform has been reported (Mukherjee and Hausman, 2004), and there are no reports of VAChT transcript isoforms. However, the highly conserved structure of the cholinergic locus (Fig. 6) makes it plausible that a similar regulation mechanism exists for the cholinergic locus in mammals and birds, which may produce as a result the dual and/or individual expression of both VAChT and ChAT proteins. A specific downregulation of VAChT expression concomitant with an increase in the expression of ChAT has been reported in neurons of the dorsal root ganglia of the chick (Corsetti et al., 2012). Therefore, it is possible that a downregulation of the cholinergic locus may occur in the lpc cells, which is specifically strong for the VAChT gene, leaving a diminished or "leaky" expression for the ChAT gene. The CHT1 gene could still be expressed in the lpc. as it is located on a different chromosome (Fig. 6C). Indeed, unpublished in situ hybridization results indicate that VAChT mRNA is

expressed in the lpc during development and becomes undetected days before hatching (R. Reyes, C. Gonzalez-Cabrera, J.C. Ferran, L. Puelles, and G. Marín, manuscript in preparation).

A higher expression in the lpc of the VAChT gene may persist at postnatal stages in other species, as illustrated by an in situ assay displayed online (ZEBrA: A Zebra Finch Expression Atlas, RRID: nif-0000–24345; http://www.zebrafinchatlas.org), which shows mild VAChT and weak VGluT2 mRNA expression in the lpc of the zebra finch. We did clone a specific probe for the VAChT mRNA of the zebra finch (unpublished results) and found an expression pattern in two adult individuals similar to that observed in the chick, albeit with a very light level of expression of VAChT in the lpc.

Thus, overall, we believe that our results consistently indicate that the VAChT mRNA expression in the lpc of the chick is heavily diminished, if not completely silenced. High levels of expression of the glutamate transporter would complement this downregulaton. A similar downregulation of VAChT might occur in species showing strong expression of VGLuT2 in the lpc, like pigeons (Islam and Atoji, 2008), whereas in other species, perhaps those with altricial development like the zebra finch, VAChT expression might remain high. Indeed, the lpc of more avian species needs to be investigated to understand the phylogenetic distribution of the VACHT/VGLuT2 phenotype. An interesting case study would be the owl, an altricial species more closely related to passerines than to pigeons and chickens (Hackett et al., 2008), whose isthmotectal-system has been intensively studied (Asadollahi et al., 2010).

VGluT2 expression in lpc neurons

The high VGluT2 mRNA expression in the lpc perikarya is in agreement with a previous report that used a different VGluT2 probe in pigeons (Islam and Atoji, 2008). The lpc axon terminals, the paintbrushes, and the presumptive presynaptic boutons were also immunoreactive to a VGluT2 antibody, strongly implying a glutamatergic identity for this nucleus. These results are also in agreement with a report by Morino et al. (1991) showing, in retinal ablated pigeons, glutamate-like immunoreactive processes in tectal layers 2 and 5, which resembled lpc axon terminals.

The distribution of VGluT2 in the chick brain corresponds with that observed in the pigeon (Islam and Atoji, 2008), which confirms the specificity of the probe used in this study, in accordance with the bioinformatics design.

An experimental demonstration of glutamate release by the lpc axon terminals would confirm the glutamatergic function; however, there are two anatomical circumstances that render this task difficult. First, the lpc axon terminals intermingle with the dense neuropil of glutamatergic retinal terminals, obscuring the interpretation of standard microdialysis experiments or local evoked potential recordings. Second, the possibility of recording intracellular postsynaptic potentials after lpc stimulation, to perform pharmacological experiments, is hampered by electron microscopic evidence indicating that the lpc axon terminals specifically terminate in the dendritic specializations of the TGC neurons (C. Gonzalez-Cabrera, F. Garrido-Charad, P. Bolam, and G. Marín, unpublished results). These dendritic specializations are characteristically arranged very far from the neural soma and presumably also receive a glutamatergic input from the retinal terminals (Tömböl and Németh, 1999). Careful experiments should overcome these difficulties, as the glutamatergic identity of the lpc is in the end a functional question.

Glutamate and acetylcholine corelease

The present results raise the possibility of a dual release of glutamate and acetylcholine by lpc neurons. Increasing evidence has demonstrated the presence of glutamate transporters in neurons previously defined as catecholaminergic, GABAergic, or cholinergic (El Mestikawy et al., 2011) strengthening the idea of neuronal cotransmission. Likewise, coexpression of VGluT2, ChAT, and VAChT mRNAs and their corresponding proteins has been reported in motor neurons of the rat spinal cord (Ichikawa et al., 1997; Herzog et al., 2004; Nishimaru et al., 2005). Finally, it has been suggested that the vesicular transporters VGluT2 and VAChT could be arranged in different compartments or act synergistically within the same synaptic vesicle (Herzog et al., 2004; El Mestikawy et al., 2011), and that the function of glutamate and acetylcholine corelease would be associated with a dual transmission of fast and slow excitatory signals, respectively (El Mestikawy et al., 2011). Our results suggest a similar expression pattern in the chicken pretectum, where the SpM nucleus expresses VACHT, ChAT, and VGluT2 mRNA and shows immunoreactivity for the ChAT protein, although it remains to be determined whether the three markers are coexpressed in the same neurons. However, this does not apply to the lpc nucleus in the chick because VGluT2 mRNA was coexpressed along with the ChAT protein, whereas the vesicular transporter for acetylcholine was undetectable. Whether minimal levels of VAChT mRNA expression, undetectable in our trials, are capable of maintaining a vesicular cholinergic function in the lpc remains an open question.

An alternative and also attractive possibility is that lpc axons corelease glutamate, via a vesicular

mechanism, and acetylcholine, via a nonvesicular mechanism. For example, a mechanism postulated for acetylcholine release in the *Torpedo* electric organ (Israël et al., 1986, 1994; Bloc et al., 1999, 2000) may depend on the mediatophore, a cytoplasmic membrane proteolipid homo-oligomer that appears to directly translocate and release acetylcholine in a calcium-dependent manner (Israël et al., 1986, 1990; Bloc et al., 1999, 2000). It is possible that a similar mechanism may operate in the Ipc cells, because the homolog protein that forms the mediatophore monomers, the *c*-subunit of the membrane domain (V0) of the vacuolar-H^+ ATPase (V-ATPase), is a highly conserved protein among vertebrates.

A final possibility is that acetylcholine accumulates in Ipc presynaptic terminals and is released, in a nonquantal mode, by the high-affinity choline uptake mechanism. Recently the involvement of the choline transporter in the Ca^{2+}-dependent nonquantal release of acetylcholine by cholinergic nerves in the guinea pig airways has been reported (Chávez et al., 2011), and therefore, the expression of the CHT1 mRNA observed in Ipc neurons could support a possible nonquantal release of acetylcholine for this nucleus.

Ipc/SLu dual effect over the TeO

If, in contrast, Ipc axons mainly release glutamate, the TeO would receive two synchronized feedbacks signals from the Ipc and SLu carried by different neurotransmitters. The tectal region receiving these signals could be envisioned as two overlapping and concentric cylindrical volumes of different diameters (Fig. 7). The Ipc and SLu neurons have relatively large visual receptive fields (RFs) (20 ± 3 degrees in diameter vs. 45 ± 15 degrees, respectively), which contrast with their restricted axon terminals in the tectum (35–50 and 120–150 μm wide, respectively). Such wide RFs and the respective homotopic feedback projections imply that any small visual stimuli will activate hundreds of Ipc and SLu neurons, whose feedback axons will encompass a large tectal area: up to approximately 4.5 mm for the SLu and 2 mm for the Ipc, considering a tectal magnification factor of about 100 μm/degree (Clarke and Whitteridge, 1976). Thus, the larger tectal column associated with the SLu feedback would contain the smaller column controlled by the Ipc, in an overlapping concentric fashion. This configuration allows us to visualize a modulatory "beam" operating in the tectum with a central glutamate-releasing column (Ipc) surrounded by a wider cholinergic column (SLu), with the former controlling the tecto-rotundal visual flow, and the latter presumably exerting a modulatory effect over other tectal circuits, perhaps descending premotor

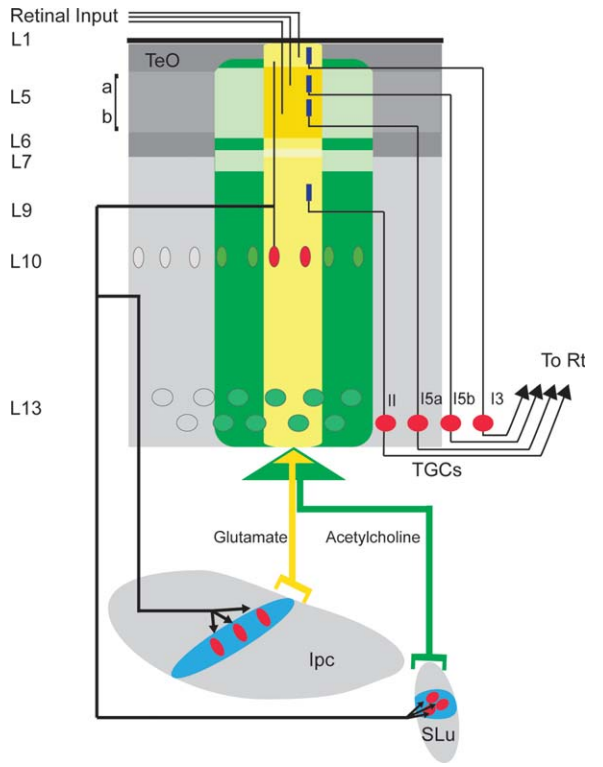

Figure 7. Schematic of a dual isthmotectal control model in chicks. The Ipc and the SLu nuclei feed back to the TeO by columnar terminal fields that ramify in the tectum, from layers 10 to 2. Color saturation represents the density of the terminals fields in the respective tectal layers. The feedbacks are displayed as two overlapping and concentric cylindrical volumes of different diameters. They establish a dual modulatory "beam" composed of a central column, mostly releasing glutamate (Ipc; yellow), controlling the tecto-rotundal visual flow, surrounded by a wider cholinergic column (SLu; green) presumably exerting a modulatory effect over other tectal circuits. TGCs, tectal ganglion cells; L1–L13, tectal layers 1–13. TGC nomenclature from Marín et al. (2003).

pathways. The Ipc axons make direct synaptic contacts on the dendritic spines of the TGCs, as suggested by the unpublished electron microscopic results mentioned above. Presumably, the sequential release of glutamate by the retinal and isthmic fibers will synergistically drive the TGC dendrites, explaining the strong control exerted by the Ipc feedback over the visual responses in all subdivisions of the rotundus (Marín et al., 2012).

In summary, the present study suggests a heterogeneous neurochemical identity for the isthmic nuclei providing a homotopic feedback projection onto the ipsilateral optic tectum of the chick, supporting the cholinergic character of the SLu and denoting a major glutamatergic function for the Ipc. These findings further suggest that the strong control exerted by the Ipc feedback on the ascending transmission of tectal visual

activity is mediated by VGluT2-positive lpc axons that would release glutamate onto their target tectal ganglion cells.

CONFLICT OF INTEREST STATEMENT

The authors have no conflicts of interest.

ROLE OF AUTHORS

All authors had full access to all the data in the study and take responsibility for the integrity of the data and the accuracy of the data analysis. Study concept and design: CG-C, AR, and GJM. Acquisition of data: CG-C, FG-C. Analysis and interpretation of data: CG-C, FG-C., and GJM. Drafting of the manuscript: CG-C and GJM. Critical revision of the manuscript for important intellectual content: CG-C, AR, and GJM. Statistical analysis: CG-C. Obtained funding: GJM and AR. Study supervision: GJM.

LITERATURE CITED

Angaut P, Repérant J. 1976. Fine structure of the optic fibre termination in the pigeon optic tectum: a Golgi and electron microscope study. Neuroscience 1:93–105.

Asadollahi A, Mysore SP, Knudsen EI. 2010. Stimulus-driven competition in a cholinergic midbrain nucleus. Nat Neurosci 13:889–895.

Atoji Y. 2011. Immunohistochemical localization of vesicular glutamate transporter 2 (vGluT2) in the central nervous system of the pigeon (*Columba livia*). J Comp Neurol. 519:2887–2905.

Bagnoli P, Fontanesi G, Alesci R, Erichsen JT. 1992. Distribution of neuropeptide Y, substance P, and choline acetyltransferase in the developing visual system of the pigeon and effects of unilateral retina removal. J Comp Neurol 318:392–414.

Bejanin S, Cervini R, Mallet J, Berrard S. 1994. A unique gene organization for two cholinergic markers, choline acetyltransferase and a putative vesicular transporter of acetylcholine. J Biol Chem 269:21944–21947.

Benowitz LI, Karten HJ. 1976. Organization of the tectofugal visual pathway in the pigeon: a retrograde transport study, J Comp Neurol 167:503–520.

Berrard S, Varoqui H, Cervini R, Israël M, Mallet J, Diebler MF. 1995. Coregulation of two embedded gene products, choline acetyltransferase and the vesicular acetylcholine transporter. J Neurochem 65:939–942.

Bischof HJ, Watanabe S. 1997. On the structure and function of the tectofugal visual pathway in laterally eyed birds. Eur J Morphol 35:246–254.

Bloc A, Bugnard E, Dunant Y, Falk-Vairant J, Israël M, Loctin F, Roulet E. 1999. Acetylcholine synthesis and quantal release reconstituted by transfection of mediatophore and choline acetyltranferase cDNAs. Eur J Neurosci 11: 1523–1534.

Bloc A, Bancila V, Israël M, Dunant Y. 2000. Reconstitution of mediatophore-supported quantal acetylcholine release. Metab Brain Dis 15:1–16.

Brock M, Nickel AC, Madziar B, Blusztajn JK, Berse B. 2007. Differential regulation of the high affinity choline transporter and the cholinergic locus by cAMP signaling pathways. Brain Res 1145:1–10.

Castell X, Diebler MF, Tomasi M, Bigari C, De Gois S, Berrard S, Mallet J, Israël M, Dolezal M. 2002. More than one way to toy with ChAT and VAChT. J Physiol Paris 96:61–72.

Castell X, Cheviron N, Barnier JV, Diebler MF. 2003. Exploring the regulation of the expression of ChAT and VAChT genes in NG108-15 cells: implication of PKA and PI3K signaling pathways. Neurochem Res 28:557–564.

Cervini R, Houhou L, Pradat PF, Bejanin S, Mallet J, Berrard S. 1995. Specific vesicular acetylcholine transporter promoters lie within the first intron of the rat choline acetyltransferase gene. J Biol Chem 270:24654–24657.

Chávez J, Vargas MH, Cruz-Valderrama JE, Montaño LM. 2012. Non-quantal release of acetylcholine in guinea-pig airways: role of choline transporter. Exp Physiol 96:460–467.

Clarke PG, Whitteridge D. 1976. The projection of the retina, including the 'red area' on to the optic tectum of the pigeon. Q J Exp Physiol Cogn Med Sci 61:351–358.

Corsetti V, Mozzetta C, Biagioni S, Augusti Tocco G, Tata AM. 2012. The mechanisms and possible sites of acetylcholine release during chick primary sensory neuron differentiation. Life Sci 91:783–788.

Cuénod, M, Sandri, C, Akert, K. 1970. Enlarged synaptic vesicles as an early sign of secondary degeneration in the optic nerve terminals of the pigeon. J Cell Sci 6: 605–613.

Domenici L, Waldvogel HJ, Matute C, Streit P. 1988. Distribution of GABA-like immunoreactivity in the pigeon brain. Neuroscience 25:931–950.

El Mestikawy S, Wallén-Mackenzie A, Fortin GM, Descarries L, Trudeau LE. 2011. From glutamate co-release to vesicular synergy: vesicular glutamate transporters. Nat Rev Neurosci 12:204–216.

Erickson JD, Varoqui H, Schafer MK, Modi W, Diebler MF, Weihe E, Rand J, Eiden LE, Bonner TI, Usdin TB. 1994. Functional identification of a vesicular acetylcholine transporter and its expression from a ''cholinergic'' gene locus. J Biol Chem 269:21929–21932.

Felix D, Wu GY, Wang SR. 1994. GABA as an inhibitory transmitter in the pigeon isthmo-tectal pathway. Neurosci Lett 169:212–214.

Fremeau RT Jr, Voglmaier S, Seal RP, Edwards RH. 2004. VGLUTs define subsets of excitatory neurons and suggest novel roles for glutamate. Trends Neurosci 27:98–103.

Goddard CA, Sridharan D, Huguenard JR, Knudsen EI. 2012. Gamma oscillations are generated locally in an attention-related midbrain network. Neuron 73:567–580.

Goddard CA, Mysore SP, Bryant AS, Huguenard JR, Knudsen EI. 2014. Spatially reciprocal inhibition of inhibition within a stimulus selection network in the avian midbrain. PLoS One 9:e85865.

Gray EG, Hamlyn LH. 1962. Electron microscopy of experimental degeneration in the avian optic téctum. J Anat 96:309–316.

Gundersen HJ, Bagger P, Bendtsen TF, Evans SM, Korbo L, Marcussen N, Moller A, Nielsen K, Nyengaard JR, Pakkenberg B, Sorensen FB, Vesterby A, West MJ. 1988. Acta Pathol Microbiol Immunol Scand 96:857–881.

Güntürkün O, Remy, M. 1990. The topographical projection of the nucleus isthmi pars parvocellularis (Ipc) onto the tectum opticum in the pigeon. Neurosci Lett 111:18–22.

Hackett SJ, Kimball RT, Reddy S, Bowie RCK, Braun EL, Braun MJ, Chojnowski JL, Cox WA, Han KL, Harshman J, Huddleston CJ, Marks BD, Miglia KJ, Moore WS, Sheldon FH, Steadman DW, Witt CC, Yuri T. 2008. A

phylogenomic study of birds reveals their evolutionary history. Science 320:1763–1768.

Hayes BP, Webster KE. 1975. An electron microscope study of the retino-receptive layers of the pigeon optic tectum. J Comp Neurol 162:447–466.

Hellmann, B, Güntürkün, O. 2001. Structural organization of parallel information processing within the tectofugal visual system of the pigeon. J Comp Neurol 429:94–112.

Herzog E, Landry M, Buhler E, Bouali-Benazzouz R, Legay C, Henderson CE, Nagy F, Dreyfus P, Giros B, El Mestikawy S. 2004. Expression of vesicular glutamate transporters, VGluT1 and VGluT2, in cholinergic spinal motoneurons. Eur J Neurosci 20:1752–1760.

Hunt SP, Kunzle H. 1976. Observations on the projections and intrinsic organization of the pigeon optic tectum: an autoradiographic study based on anterograde and retrograde, axonal and dendritic flow. J Comp Neurol 170: 173–190.

Hunt, SP, Webster, KE. 1975. The projection of the retina upon the optic tectum of the pigeon. J Comp Neurol 162:433–446.

Hunt, SP, Streit, P, Künzle, H, Cuénod, M. 1977. Characterization of the pigeon isthmo-tectal pathway by selective uptake and retrograde movement of radioactive compounds and by Golgi-like horseradish peroxidase labeling. Brain Res 129:197–212.

Ichikawa T, Ajiki K, Matsuura J, Misawa H. 1997. Localization of two cholinergic markers, choline acetyltransferase and vesicular acetylcholine transporter in the central nervous system of the rat: in situ hybridization histochemistry and immunohistochemistry. J Chem Neuroanat 13:23–39.

Islam, MR, Atoji, Y. 2008. Distribution of vesicular glutamate transporter 2 and glutamate receptor 1 mRNA in the central nervous system of the pigeon (*Columba livia*). J Comp Neurol 511:658–677.

Israël M, Morel N, Lesbats B, Birman S, Manaranche R. 1986. Purification of a presynaptic membrane protein that mediates a calcium-dependent translocation of acetylcholine. Proc Natl Acad Sci U S A 83:9226–9230.

Israël M, Lesbats B, Sbia M, Morel N. 1990. Acetylcholine translocating protein: mediatophore at rat neuromuscular synapses. J Neurochem 55:1758–1762.

Israël M, Lesbats B, Synguelakis M, Joliot A. 1994. Acetylcholine accumulation and release by hybrid NG108-15, glioma and neuroblastoma cells—role of a 16kDa membrane protein in release. Neurochem Int 25:103–109.

Karten HJ, Revzin AM. 1966. The afferent connections of the nucleus rotundus in the pigeon. Brain Res 2:368–377.

Karten HJ, Cox K, Mpodozis J. 1997. Two distinct populations of tectal neurons have unique connections within the retinotectorotundal pathway of the pigeon (*Columba livia*). J Comp Neurol 387:449–465.

Knudsen E. 2007. Fundamental components of attention. Annu Rev Neurosci 30:57–78.

Liu Y, Krantz DE, Waites C, Edwards RH. 1999. Membrane trafficking of neurotransmitter transporters in the regulation of synaptic transmission. Trends Cell Biol 9:356–363.

Luksch H, Cox K, Karten HJ. 1998. Bottlebrush dendritic endings and large dendritic fields: motion-detecting neurons in the tectofugal pathway. J Comp Neurol 396:399–414.

Luksch H, Karten HJ, Kleinfeld D, Wessel R. 2001. Chattering and differential signal processing in identified motion-sensitive neurons of parallel visual pathways in the chick tectum. J Neurosci 21:6440–6446.

Maczko KA, Knudsen PF, Knudsen EI. 2006. Auditory and visual space maps in the cholinergic nucleus isthmi pars parvocellularis of the barn owl. J Neurosci 26:12799–12806.

Mallet J, Houhou L, Pajak F, Oda Y, Cervini R, Bejanin S, Berrard S. 1998. The cholinergic locus: ChAT and VAChT genes. J Physiol Paris 92:145–147.

Marín G, Letelier JC, Henny P, Sentis E, Farfán G, Fredes F, Pohl N, Karten H, Mpodozis J. 2003. Spatial organization of the pigeon tectorotundal pathway: an interdigitating topographic arrangement. J Comp Neurol 458:361–380.

Marín G, Mpodozis, J, Sentis, E, Ossandon, T, Letelier, JC. 2005. Oscillatory bursts in the optic tectum of birds represent re-entrant signals from the nucleus isthmi pars parvocellularis. J Neurosci 25:7081–7089.

Marín G, Salas, C, Sentis, E, Rojas, X, Letelier, JC, Mpodozis, J. 2007. A cholinergic gating mechanism controlled by competitive interactions in the optic tectum of the pigeon. J Neurosci 27:8112–8121.

Marín G, Duran E, Morales C, González-Cabrera C, Sentis E, Mpodozis J, Letelier JC. 2012. Attentional capture? Synchronized feedback signals from the isthmi boost retinal signals to higher visual areas. J Neurosci 32:1110–1122.

Medina L, Reiner A. 1994. Distribution of choline acetyltransferase immunoreactivity in the pigeon brain. J Comp Neurol 342:497–537.

Morino P, Bahro M, Cuenod M, Streit P. 1991. Glutamate-like Immunoreactivity in the pigeon optic tectum and effects of retinal ablation. Eur J Neurosci 3:366–378.

Mpodozis J, Letelier JC, Maturana H. 1995. Nervous system as a closed neuronal network: behavioral and cognitive consequences. Lecture Notes Comput Sci 930:130–136.

Mpodozis J, Cox K, Shimizu T, Bischof HJ, Woodson W, Karten HJ. 1996. GABAergic inputs to the nucleus rotundus (pulvinar inferior) of the pigeon (*Columba livia*). J Comp Neurol 374:204–222.

Mukherjee RS, Hausman RE. 2004. Cloning of chicken choline acetyltransferase and its expression in early embryonic retina. Mol Brain Res 129:54–66.

Mysore SP, Knudsen EI. 2013. A shared inhibitory circuit for both exogenous and endogenous control of stimulus selection. Nat Neurosci 16:473–478.

Naciff JM, Misawa H, Dedman JR. 1997. Molecular characterization of the mouse vesicular acetylcholine transporter gene. Neuroreport 8:3467–3473.

Nguyen AP, Spetch ML, Crowder NA, Winship IR, Hurd PL, Wylie DR. 2004. A dissociation of motion and spatial-pattern vision in the avian telencephalon: implications for the evolution of "visual streams". J Neurosci 24:4962–4970.

Nishimaru H, Restrepo CE, Ryge J, Yanagawa Y, Kiehn O. 2005. Mammalian motor neurons corelease glutamate and acetylcholine at central synapses. Proc Natl Acad Sci U S A 102:5245–5249.

Ramón y Cajal S. 1911. Histology of the nervous system of man and vertebrates. Translated from Spanish to French by Azoulay L, from French to English by Swanson N and Swanson LW, 1995. New York: Oxford University Press.

Reubi JC, Cuénod M. 1976. Release of exogenous glycine in the pigeon optic tectum during stimulation of a midbrain nucleus. Brain Res 112:347–361.

Reperant J, Angaut P. 1977. The retinotectal projections in the pigeon. An experimental optical and electron microscope study. Neuroscience 2:119–140.

Roghani A, Feldman J, Kohan S, Shirzadi A, Gunderson C, Brecha N, Edwards R. 1994. Molecular cloning of a

putative vesicular transporter for acetylcholine. Proc Natl Acad Sci U S A 91:10620–10624.

Schütz B, Weihe E, Eiden LE. 2001. Independent patterns of transcription for the products of the rat cholinergic gene locus. Neuroscience 104:633–642.

Shimojo M, Wu D, Hersh LB. 1998. The cholinergic gene locus is coordinately regulated by protein kinase A II in PC12 cells. J Neurochem 71:1118–1126.

Sorenson, E, Parkinson, D, Dahl, J, Chiappinelli, V. 1989. Immunohistochemical localization of choline acetyltransferase in the chicken mesencephalon. J Comp Neurol 281:641–657.

Sun Z, Wang HB, Laverghetta A, Yamamoto K, Reiner A. 2005. The distribution and cellular localization of glutamic acid decarboxylase-65 (GAD65) mRNA in the forebrain and midbrain of domestic chick. J Chem Neuroanat 29:265–281.

Tömböl T, Németh A. 1999. Direct connections between dendritic terminals of tectal ganglion cells and glutamate-positive terminals of presumed optic fibres in layers 4–5 of the optic tectum of *Gallus domesticus*. A light- and electron microscopic study. Neurobiology (Bp) 7:45–67.

Veenman CL, Reiner A. 1994. The distribution of GABA-containing perikarya, fibers, and terminals in the forebrain and midbrain of pigeons, with particular reference to the basal ganglia and its projection targets. J Comp Neurol 339:209–250.

Wang SR, Wang YC, Frost BJ. 1995. Magnocellular and parvocellular divisions of pigeon nucleus isthmi differentially modulate visual responses in the tectum. Exp Brain Res 104:376–384.

Wang Y, Xiao J, Wang SR. 2000. Excitatory and inhibitory receptive fields of tectal cells are differentially modified by magnocellular and parvocellular divisions of the pigeon nucleus isthmi. J Comp Physiol A 186:505–511.

Wang Y, Major DE, Karten HJ. 2004. Morphology and connections of nucleus *isthmi pars magnocellularis* in chicks (*Gallus gallus*). J Comp Neurol 469:275–297.

Wang Y, Luksch H, Brecha NC., Karten HJ. 2006. Columnar projections from the cholinergic nucleus isthmi to the optic tectum in chicks (*Gallus gallus*): a possible substrate for synchronizing tectal channels. J Comp Neurol 494:7–35.

Weihe E, Schafera M, Schiitza B, Anlaufa M, Depboylua C, Bretta C, Chenb L, Eidenb LE. 1998. From the cholinergic gene locus to the cholinergic neuron. J Physiol Paris 92:385–388.

Wylie DR, Gutiérrez-Ibáñez C, Pakan JMP, Iwaniuk AN. 2009. The optic tectum of birds: mapping our way to understanding visual processing. Can J Exp Psychol 63:328–338.